

# Fractional Quantum Hall States at $1/3$ and $5/2$ Filling: the Density-Matrix Renormalization Group Calculations

Jize Zhao and D. N. Sheng

*Department of Physics and Astronomy, California State University, Northridge, California 91330, USA*

F. D. M. Haldane

*Department of Physics, Princeton University, Princeton, NJ 08544*

(Dated: April 15, 2019)

In this paper, the density-matrix renormalization group method is employed to investigate the fractional quantum Hall effect at filling fractions  $\nu = 1/3$  and  $5/2$ . We first present benchmark results at both filling fractions for large system sizes to show the accuracy as well as the capability of the numerical algorithm. Furthermore, we show that by keeping a large number of basis states, one can also obtain accurate entanglement spectrum at  $\nu = 5/2$  for large system with electron number up to  $N_e = 34$ , much larger than systems previously studied. Based on a finite-size scaling analysis, we demonstrate that the entanglement gap defined by Li and Haldane [1] is finite in the thermodynamic limit, which characterizes the topological order of the FQHE state.

PACS numbers: 73.43.Cd, 73.43.Lp

## I. INTRODUCTION

In condensed matter physics, one of the major challenges is to understand the strong correlation effect in interacting electron systems. The fractional quantum Hall effect (FQHE) systems<sup>2</sup> are primary examples, where new quantum phases emerge with fractional quasiparticle excitations<sup>3</sup> resulting from such effect. Theoretical understanding<sup>3-7</sup> of the odd denominator FQHE states in the lowest Landau level ( $n = 0$ ) has been fully developed soon after the experimental discovery<sup>2</sup>. The even denominator<sup>8</sup> quantum Hall states in second Landau level ( $n = 1$ ) appear to demonstrate complex nature beyond the understanding of a unified theory, which are under intensive studies<sup>9-20</sup>.

Theoretical approaches<sup>7,10-12,16</sup> have predicted a variety of possible candidate states for even-denominator quantum Hall systems, some of which are exotic in nature with quasiparticles obeying non-Abelian statistics. However, very often such theories cannot provide solutions to microscopic theoretical models describing realistic electron systems. In this aspect, computational studies have played an important role to determine the quantum state for such systems. Pioneer works have been done using exact diagonalization (ED) method to establish the nearly perfect overlap of the Laughlin wave function with the exact ground state wavefunction of small electron systems and provide microscopic understanding of the nature of the FQHE<sup>4,6,9</sup>. In recent years, ED has been widely used to study FQHE for pure systems<sup>20-24</sup> as well as disordered systems<sup>25</sup> to probe the nature of various quantum phases and transitions. It has been recently established that ED can also be used to identify the topological nature of a quantum phase based on entanglement entropy and the entanglement spectrum of the quantum systems<sup>1,26-29</sup>. However, since the Hilbert space increases exponentially with the system size, ED is limited to systems with a small electron number (typi-

cally restricted to electron number  $N_e = 14 \sim 20$  depending on the Landau level filling number). This limitation becomes a severe problem when the finite-size effect is strong, which is usually the case for quantum states in the higher Landau levels or with even denominator filling fractions.

The density-matrix renormalization group (DMRG) developed by White is an unbiased powerful method for studying interacting systems with accuracy controlled by the number of states kept in DMRG blocks<sup>30,31</sup>. It has been widely applied to quasi-one-dimensional systems, providing essentially exact results for spin or electron systems. However, its application to two-dimensional systems remains to be quite challenging. It is generally believed that the number of states desired to be kept in each block should grow exponentially with the increase of the system width to catch up the entanglement entropy between two coupled blocks<sup>32</sup>. Nevertheless, FQHE systems can be modeled as one dimensional system with long-range Coulomb interaction, which may become accessible using current computational power. Shibata and Yoshioka made the first attempt to develop DMRG algorithm to study quantum Hall systems in torus geometry<sup>33</sup> about ten years ago. Various fillings have been studied<sup>34</sup> by keeping hundreds of states obtaining useful information of larger systems at integer fillings or for compressible states. Recently, a great progress has been made by Feiguin *et al.*<sup>35,36</sup> developing new DMRG algorithm keeping up to 5,000 states in their work. The hard problems of the incompressible FQHE at  $\nu = 1/3$  and  $5/2$  have been extensively studied, providing convincing high accuracy ground state and excited state results for larger system sizes up to 20 and 26 electrons at  $\nu = 1/3$  and  $5/2$ , respectively. Moreover, DMRG has also been applied to study bosonic quantum Hall effect<sup>37</sup>.

In this paper, we study FQHE systems based on our newly developed DMRG code, which substantially improves the accuracy of the results through keeping more

states and managing DMRG process with higher efficiency. The benchmark results and error analysis are presented for  $\nu = 1/3$  and  $5/2$ . For the same system sizes studied before, we reduce the error substantially especially for  $5/2$  systems, while we access systems with more electrons with high accuracy. We also obtain accurate entanglement spectra for  $\nu = 5/2$  systems, which identify the topological order at larger system sizes. The entanglement gap for  $\nu = 5/2$  FQHE first revealed by Li and Haldane<sup>1</sup> based on ED calculation, remains finite in the thermodynamic limit established through finite-size scaling analysis.

## II. HAMILTONIAN AND METHOD

In this paper, we study the FQHE in the spherical geometry<sup>4</sup>, where electrons are confined on the surface of a sphere with radius  $R$ . The total magnetic flux through the spherical surface  $4\pi R^2 B$  are quantized to be an integer  $2S$  multiple of the flux quanta. Assuming that electrons are polarized by the magnetic field and neglecting the Landau level mixing, the Hamiltonian in the spherical geometry can be written as

$$\mathcal{H} = \frac{1}{2} \sum_{m_1, m_2, m_3, m_4} \langle m_1 m_2 | V | m_3 m_4 \rangle a_{m_1}^\dagger a_{m_2}^\dagger a_{m_3} a_{m_4} \quad (1)$$

where the  $m_i$  is the z-component of the angular momentum and  $m_i = -L, -L+1, \dots, L$ , with  $L = S + n$  being the total angular momentum and  $n$  is the Landau level index.  $V$  is the Coulomb interaction between electrons in units of  $\frac{e^2}{l_0}$ , with  $l_0 = \sqrt{\hbar c / e B}$  being the magnetic length. In the next sections, we also use the renormalized magnetic length  $l_0^{(\infty)}$  to rescale the energy unit if it is mentioned explicitly<sup>22,24</sup>.  $a_m(a_m^\dagger)$  is the annihilation (creation) operator at the orbital  $m$ . The problem can be naturally studied using the DMRG method in momentum space<sup>38</sup> as nonzero matrix elements in the Eq. (1) only exist between orbitals satisfying the angular momentum conservation relation  $m_1 + m_2 = m_3 + m_4$ .

In our DMRG process, we arrange the  $2L + 1$  orbitals into a one-dimensional chain, corresponding to states with z-component of the angular momentum  $m$  taking different values  $L, L-1, \dots, -L+1, -L$  from left to right. In the initial process, we start from a small system with two blocks (each block has only one orbital) and two single orbitals in the middle forming a configuration  $B_L \bullet \bullet B_R$ . We write the Hamiltonian (1) terms using the product of block operators and single site operators<sup>30,31,38</sup> and diagonalize the Hamiltonian to obtain the ground state. The reduced density matrix is formed and diagonalized by following the standard DMRG<sup>30</sup> procedure. A new block  $B_L$  ( $B_R$ ) is formed by including the single site into the current block. This procedure is repeated until the 1D chain grows into the desired system size with  $2L+1$  orbitals. From this point, the finite-size sweeping algorithm is employed until we obtain the converged results.

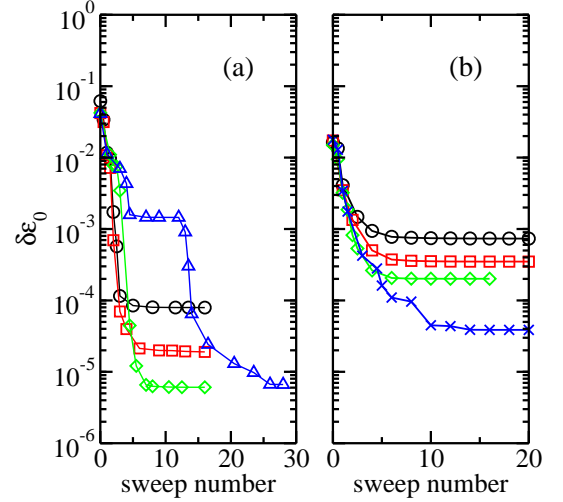


FIG. 1: (color online) Error in the ground state energy per electron  $\delta\epsilon_0$  is shown at (a)  $\nu = 1/3$  and  $N_e = 20$ , with 1,600 ( $\circ$ ), 3,200 ( $\square$ ), and 5,000 ( $\diamond$ ) states kept, respectively. The triangle data (obtained by keeping 5,000 states) illustrate a situation where DMRG runs into a local minimum during initial 12 sweeps, see text for details. The reference ground state energy is -0.4210509, obtained by DMRG with at most 24,000 states kept. (b)  $\nu = 5/2$  and  $N_e = 24$  with 1,600 ( $\circ$ ), 3,200 ( $\square$ ), and 5,000 ( $\diamond$ ) states kept, respectively. The data showed by  $\times$  are obtained by keeping 8,000, 10,000 and 14,000 states for each 4 sweeps starting from the first sweep, and 16,000 states for the rest of sweeps. The reference ground state energy is -0.3876150, obtained by DMRG with at most 30,000 states kept.

Using our momentum space DMRG, the Hamiltonian (1) is diagonalized in the sector with fixed electron number  $N_e$  and the total angular momentum z-component  $L_z$ . In the initial process of the calculation, only a small fraction of the momentum sectors in each block contributes significantly to the ground state wavefunction. States in other sectors, which have zero eigenvalues in reduced density matrix, are being discarded. However, these discarded states may become also important to the ground state wavefunction in the later stage when system grows to the full length<sup>38</sup>. To overcome this problem, we need to keep additional sectors from very beginning. For this purpose, we set a minimum number of sectors  $N_{sec}^{min}$ , which in practice is about 3  $\sim$  5 times larger than the number of sectors after convergence. In each of selected sectors, we keep at least two states with largest eigenvalues in the sector. The remaining states are selected following the standard DMRG procedure to minimize the truncation error. In the sweep process,  $N_{sec}^{min}$  is gradually decreased as a function of sweep number.

In Fig. 1(a), we show the error of the obtained ground state energy per electron at  $\nu = 1/3$  for different number of states kept in each block with respect to the fully converged reference energy obtained by keeping much more states. A reasonable accuracy around  $10^{-4}$  is reached with the electron number  $N_e = 20$  (bigger than the

largest ED size by six electrons) by keeping only 1,600 states, while we achieve the accuracy of  $6 \times 10^{-6}$  by keeping 5,000 states. However, the convergence becomes more difficult for  $\nu = 5/2$  system, as we show in Fig. 1(b). For  $N_e = 24$  (bigger than the largest ED size by four electrons), with  $m = 5,000$  states kept, the accuracy we can achieve is about  $2 \times 10^{-4}$ , comparable with the results obtained by Feiguin et al<sup>35</sup>. Further increasing the number of states kept to 16,000, we are able to reduce the error by a factor of five.

Controlling  $N_{sec}^{min}$  also allows us to overcome the local minimum trapping, which could trap the DMRG obtained state in an excited state. As we show in Fig. 1(a) by triangles, the energy is pinned to a local minimum from the fifth sweep to twelfth sweeps, and the error is much larger than the data showed by  $\diamond$  starting from a different initial state. To overcome the problem, we simply increase  $N_{sec}^{min}$  at the twelfth sweep to allow a larger number of sectors to get into the Hilbert space. These additional sectors bring in significant quantum fluctuations and eventually get the state out of the local minimum.

### III. RESULTS

#### A. Ground state energies at $\nu = 1/3$ and $5/2$

To demonstrate the accuracy of our DMRG calculations, we have obtained the ground state energy for system up to 24 electrons at  $\nu = 1/3$  by keeping up to 20,000 states, which leads to a truncation error smaller than  $10^{-11}$  in the final sweep. The maximum dimension of the Hilbert space diagonalized is of the order of  $2 \times 10^7$ . In Fig. 2, we show the ground state energy

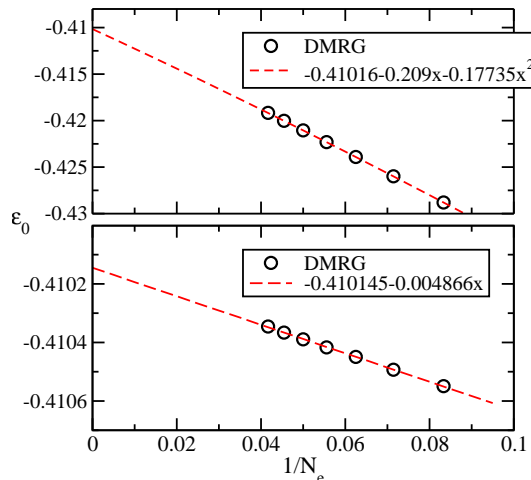


FIG. 2: (color online) (a) Finite-size scaling of ground state energy per electron at  $\nu = 1/3$  with a quadratic extrapolation. (b) Finite-size scaling of ground state energy per electron at  $\nu = 1/3$  with a linear extrapolation. Energy unit is renormalized by  $l_0^{(\infty)}$ . The error bars in both figures are much smaller than the size of the symbols.

as a function of  $1/N_e$  with  $2L = 3(N_e - S_0)$ , where a shift of  $S_0 = 1$  has been used. In the upper panel numerical data are extrapolated to thermodynamic limit by a quadratic function of  $1/N_e$ , which gives the ground state energy per electron  $\epsilon_0 = -0.41016(2)$ . In the lower panel we rescale the energy by the renormalized magnetic length<sup>22,24</sup> and extrapolate the numerical data linearly, leading to  $\epsilon_0 = -0.410145(15)$  demonstrating consistency between two extrapolating methods. While our results are essentially in agreement with previous results recently obtained by Feiguin et al<sup>35</sup> using DMRG method, our accuracy is improved by keeping much more states, which opens opportunity for studying larger systems. Now we turn to the study of the FQHE at  $\nu = 5/2$ . We calculate the ground state energy up to  $N_e = 34$  electrons, with at most 24,000 states kept. The maximum dimension of the space we diagonalize is around  $3.5 \times 10^7$ . The truncation error is of the order of  $10^{-7}$  indicating larger error in DMRG comparing to  $\nu = 1/3$  case due to smaller gap separating the excited states and the ground state. The data at the largest system size were obtained within three weeks on one 12 cores Xeon server. In upper

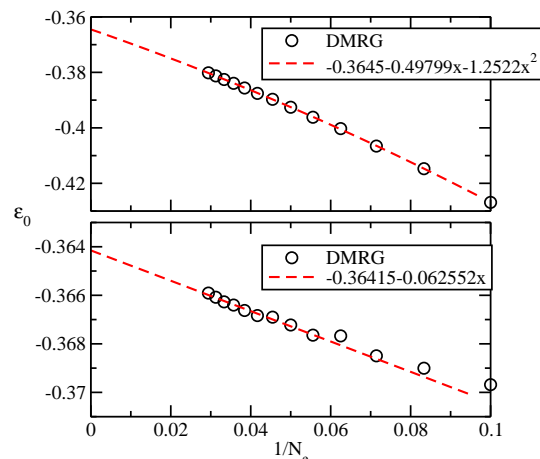


FIG. 3: (color online) (a) Finite-size scaling of the ground state energy at  $\nu = 5/2$  with a quadratic fitting. (b) Finite-size scaling of the ground state energy at  $\nu = 5/2$  with a linear fitting. Energy unit is renormalized by  $l_0^{(\infty)}$  and only  $N_e \geq 18$  is used in view of the strong finite-size oscillation.

panel of Fig. 3, we show the ground state energy  $\epsilon_0$  as a function of  $1/N_e$ . With a quadratic fitting, the extrapolated value in the thermodynamic limit is  $-0.3645(6)$ . In the lower panel, we rescale the ground state energy by the renormalized magnetic length  $l_0^{(\infty)}$  and extrapolated ground state energy is  $-0.36415(45)$  by a linear function. We further calculate the excitation gaps at  $\nu = 5/2$  up to  $N_e = 26$ , including neutral exciton gap ( $\Delta^{exc}$ ) and the charged excitation gap ( $\Delta$ ), following the definitions in Ref. 24. Some of the data are present in Table I as a function of  $N_e$ , where the excited states “aliased” to other quantum Hall states are excluded<sup>23,24</sup>. The estimated gaps in the thermodynamic limit are  $\Delta^{exc} = 0.032 \pm 0.004$

TABLE I: Excitation gaps at  $\nu = 5/2$  as a function of  $N_e$ . Some data for exciton gaps are not shown here.

$N_e$	10	14	18	22	26
$\Delta^{exc}$	0.03905	0.03981	0.03751	0.03823	0.03982
$\Delta$	0.04518	0.03934	0.03619	0.03756	0.03482

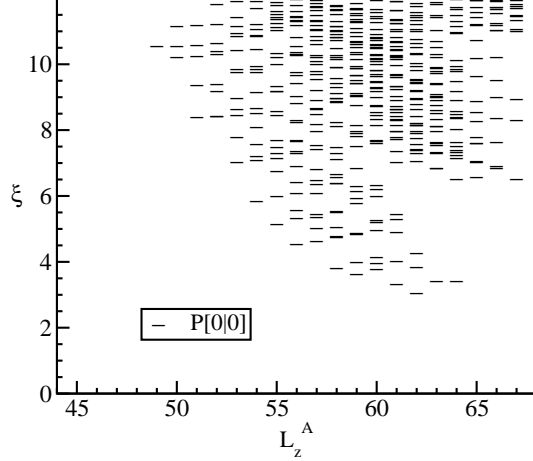


FIG. 4: The low-lying entanglement spectrum of  $N_e = 16$  for the partition  $P[0|0]$  obtained by DMRG are shown.

and  $\Delta = 0.029 \pm 0.003$ , in agreement with early result, although we observe that the strong finite-size oscillation persists even for our larger system size data.

### B. Entanglement spectrum and entanglement gaps

By dividing  $2L + 1$  orbitals into two parts,  $A$  and  $B$ , the ground state can be written, according to Schmidt decomposition, as

$$|\psi\rangle = \sum_i e^{-\xi_i/2} |\psi_A^i\rangle \otimes |\psi_B^i\rangle, \quad (2)$$

where the singular eigenvalues  $\exp(-\xi_i/2)$  obtained from diagonalizing the reduced density matrix define the entanglement spectrum  $\xi_i$ . The  $|\psi_A^i\rangle$  and  $|\psi_B^i\rangle$  are the orthogonal basis states of part  $A$  and  $B$ , respectively. In the pioneer work of Li and Haldane<sup>1</sup>, the entanglement spectrum for system at  $\nu = 5/2$  has been analyzed based on exact diagonalization calculation up to  $N_e = 16$  electrons. The obtained entanglement spectrum show the same structure as the conformal field theory (CFT) for the Moore-Read state, below an entanglement gap while the non-CFT type of spectrum exist above the gap. Therefore, the entanglement spectrum reveals more information than the entanglement entropy<sup>26,27</sup>. Although the entanglement spectrum and entropy are naturally obtained in DMRG, they are much harder to converge<sup>39</sup> than the ground state energy. In

the following, we demonstrate the success of our DMRG calculations in this aspect by keeping up to 24,000 states.

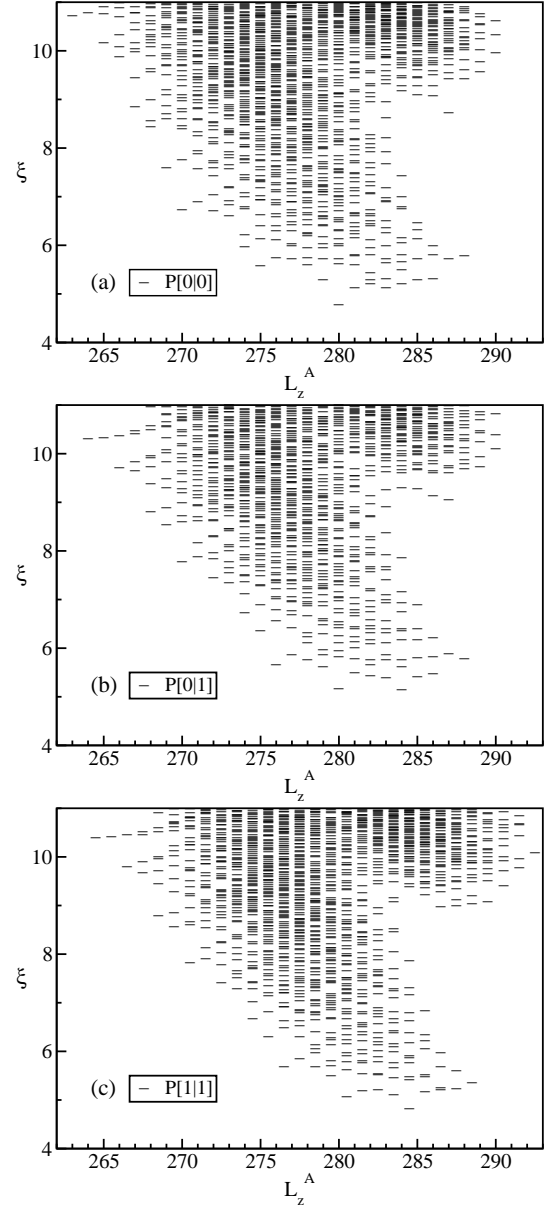


FIG. 5: The low-lying entanglement spectra of  $N_e = 34$  are shown for three partitions  $P[0|0]$ ,  $P[0|1]$  and  $P[1|1]$ .

We note that our two parts of system  $A$  and  $B$  used for Eq. (2) include the single site defined for the DMRG process, thus, the quantum numbers from both parts satisfy the equations  $N_e^A + N_e^B = N_e$  and  $L_z^A + L_z^B = 0$  (the ground state for  $5/2$  FQHE has total  $L_z = 0$ ). The entanglement spectrum can be labeled by  $N_e^A$  and  $L_z^A$  in part  $A$ . We recall that<sup>1,29</sup> for the ground state at  $\nu = 5/2$ , the highest-density “MR root configuration” has a pattern of “11001100...110011” corresponding to the “generalized Pauli principle” that no group of 4 consecutive orbits contains more than 2 particles. Conse-

quently, there are three distinct ways of partitioning the orbits as between two zeros, between zero and one, and between two ones. These three different partitions of the root configuration, identified as  $P[0|0]$ ,  $P[0|1]$ , and  $P[1|1]$  can be easily obtained in the sweeping process<sup>30</sup> during the DMRG calculations.

To check the accuracy we compare the entanglement spectrum obtained by DMRG with that obtained by ED for  $N_e = 16$  for the partition  $P[0|0]$ , as shown in Fig. 4. DMRG results precisely reproduce ED results<sup>1</sup>. Next, we turn to consider larger size. In Fig. 5, we show the entanglement spectra of three partitions for  $N_e = 34$ . The low-lying spectra have the identical counting structure viewing as a function of the  $\Delta L = L_{z,max}^A - L_z^A$  (here the  $L_{z,max}^A = 288$  for the partition  $P[0|0]$ ) comparing to the results presented by Li and Haldane [1], establishing the identical topological order as in the Moore-Read state at this larger system size. Furthermore, the same spectrum structure has also been obtained for a wide range of even electron numbers  $8 \leq N_e \leq 34$ .

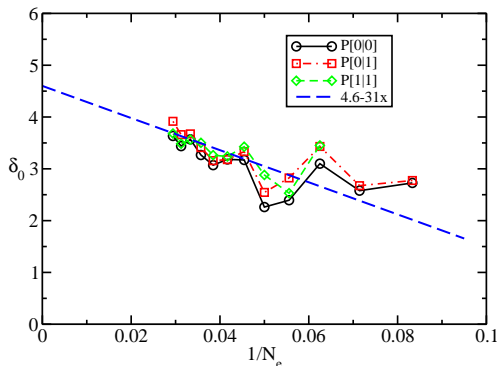


FIG. 6: (color online). Entanglement gap at  $\Delta L = 0$  vs  $1/N_e$  for three different partitions. Dashed blue line is a linear fit for  $N_e \geq 16$ .

Identifying whether entanglement gaps persist in the thermodynamic limit is particularly important for the es-

tablishment of the topologically ordered state in such a system. This is different from the finite-size wavefunction overlaps between the wavefunction of a realistic interacting system and model wave-functions (Laughlin or Moore-Read wavefunctions) as such overlaps have to go to zero with the increase of the system size related to the presence of the generic entanglement spectrum in the system. Here we have obtained the entanglement spectrum gap for a relatively large range of the system sizes, which allows us to extrapolate the gap to the thermodynamic limit. In Fig. 6, we show the entanglement gap  $\delta_0$  at  $\Delta L = 0$  as a function of  $1/N_e$  for three partitions. Entanglement gap oscillate strongly for small sizes, and the oscillation magnitude becomes smaller as  $N_e$  increases. Moreover, the lines for the three partitions almost fall into one curve. A linear fitting yields the entanglement gap  $\delta_0 = 4.6 \pm 0.6$  in the thermodynamic limit and thus our work confirms the conjecture of a finite entanglement gap made by Li and Haldane<sup>1</sup>.

#### IV. CONCLUSIONS

We have presented systematic numerical results obtained by a newly developed DMRG program for FQHE systems. We have substantially improved the DMRG algorithm and obtained accurate results for ground state energy and excitation gap for larger systems than previous works by ED and DMRG at  $\nu = 1/3$  and  $5/2$ . In particular, we demonstrate the robustness of the low-lying CFT entanglement spectrum for large system size with  $N_e = 34$  and the finite entanglement gap in the thermodynamic limit at  $\nu = 5/2$  based on finite-size scaling.

J. Zhao is grateful to H. T. Lu and C. T. Shi for helpful discussion. This work is supported by US DOE Office of Basic Energy Sciences under grant DE-FG02-06ER46305 (DNS), the NSF grants DMR-0611562, DMR-0906816 (JZ), and MRSEC Grant DMR-0819860 (FDMH).

- <sup>1</sup> Hui Li and F. D. M. Haldane, Phys. Rev. Lett. **101**, 010504 (2008).
- <sup>2</sup> D. C. Tsui, H. L. Stormer, and A. C. Gossard, Phys. Rev. Lett. **48**, 1559 (1982).
- <sup>3</sup> R. B. Laughlin, Phys. Rev. Lett. **50**, 1395 (1983).
- <sup>4</sup> F. D. M. Haldane, Phys. Rev. Lett. **51**, 605 (1983).
- <sup>5</sup> B. I. Halperin, Phys. Rev. Lett. **52**, 1583 (1984).
- <sup>6</sup> D. Yoshioka, B. I. Halperin, and P. A. Lee, Phys. Rev. Lett. **18**, 1219 (1983).
- <sup>7</sup> J. K. Jain, Phys. Rev. Lett. **63**, 199 (1989).
- <sup>8</sup> R. Willett, J. P. Eisenstein, H. L. Stormer, D. C. Tsui, A.C. Gossard, and J. H. English, Phys. Rev. Lett. **59**, 1776 (1987); J. Einstein *et al*, Phys. Rev. Lett. **61**, 997 (1988).
- <sup>9</sup> F. D. M. Haldane and Rezayi, Phys. Rev. Lett. **60**, 956 (1988).
- <sup>10</sup> G. Moore and N. Read, Nucl. Phys. **B360**, 362 (1991).

- <sup>11</sup> B. Blok and X. G. Wen, Phys. Rev. B **42**, 8145 (1990), X. G. Wen and A. Zee, Phys. Rev. B **46**, 2290 (1992).
- <sup>12</sup> E. Fradkin, C. Nayak, A. Tsvelik, and F. Wilczek, Nucl. Phys. **B516**, 704 (1998).
- <sup>13</sup> N. Read and E. Rezayi, Phys. Rev. B **59**, 8084 (1999).
- <sup>14</sup> J. S. Xia *et al*, Phys. Rev. Lett. **93**, 177809 (2004); G. Gervais *et al*, Phys. Rev. Lett. **93**, 266804 (2004).
- <sup>15</sup> S. Das Sarma, M. Freedman, and C. Nayak, Phys. Rev. Lett. **94**, 166802 (2005).
- <sup>16</sup> C. Nayak, S. H. Simon, A. Stern, M. Freedman, and S. Das Sarma, Rev. Mod. Phys. **80**, 1083 (2008).
- <sup>17</sup> M. Levin, B. I. Halperin, and B. Rosenow, Phys. Rev. Lett. **99**, 236806 (2007).
- <sup>18</sup> S. S. Lee, S. Ryu, C. Nayak, and M. P. A. Fisher, Phys. Rev. Lett. **99**, 236807 (2007).
- <sup>19</sup> Michael R. Peterson, Kwon Park, and S. Das Sarma, Phys.

- Rev. Lett. **101**, 156803 (2008).
- <sup>20</sup> H. Wang, D.N. Sheng, and F.D.M. Haldane, Phys. Rev. B **80**, 241311 (2009).
- <sup>21</sup> G. Fano, F. Ortolani, and E. Colombo, Phys. Rev. B **34**, 2670 (1986).
- <sup>22</sup> N. d'Ambrumenil and R. Morf, Phys. Rev. B **40**, 6108 (1989).
- <sup>23</sup> R. H. Morf, Phys. Rev. Lett. **80**, 1505 (1998).
- <sup>24</sup> R. H. Morf, N. d'Ambrumenil, and S. Das Sarma, Phys. Rev. B **66**, 075408 (2002).
- <sup>25</sup> Xin Wan, D. N. Sheng, E. H. Rezayi, Kun Yang, R. N. Bhatt, and F. D. M. Haldane, Phys. Rev. B **72**, 075325 (2005).
- <sup>26</sup> M. Haque, O. Zozulya, and K. Schoutens, Phys. Rev. Lett. **98**, 060401 (2007).
- <sup>27</sup> B. A. Friedman and G. C. Levine, Phys. Rev. B **78** 035320 (2008).
- <sup>28</sup> O. S. Zozulya, Masudul Haque, and N. Regnault, Phys. Rev. B **79**, 045409 (2009).
- <sup>29</sup> B. A. Bernevig and F. D. M. Haldane, Phys. Rev. Lett. **100**, 246802 (2008); *ibid.* 102, 066802 (2009).
- <sup>30</sup> S. R. White, Phys. Rev. Lett. **69**, 2863 (1992); Phys. Rev. B **48**, 10345 (1993).
- <sup>31</sup> U. Schollwöck, Rev. Mod. Phys. **77**, 259 (2005).
- <sup>32</sup> F. Verstraete, and J. I. Cirac, arXiv:cond-mat/0407066.
- <sup>33</sup> N. Shibata and D. Yoshioka, Phys. Rev. Lett. **86**, 5755 (2001).
- <sup>34</sup> See, for example, N. Shibata, Prog. Theor. Phys. Supplement No. 176 (2008) pp. 182-202.
- <sup>35</sup> A. E. Feiguin, E. Rezayi, C. Nayak, and S. Das Sarma, Phys. Rev. Lett. **100**, 166803 (2008).
- <sup>36</sup> A. E. Feiguin, E. Rezayi, Kun Yang, C. Nayak, and S. Das Sarma, Phys. Rev. B **79**, 115322 (2009).
- <sup>37</sup> D. L. Kovrizhin, Phys. Rev. B **81**, 125130 (2010).
- <sup>38</sup> T. Xiang, Phys. Rev. B **53**, R10445 (1996).
- <sup>39</sup> D. N. Sheng, Olexei I. Motrunich, and Matthew P. A. Fisher, Phys. Rev. B **79**, 205112 (2009).